INVITED PAPER *Special Section on Electronic Displays*

Electrically Controllable Light Scattering Properties of Nematic Liquid Crystal/Polyfluorene Gel Devices

Asuka YAGI[†], ***Nonmember***, **Michinori HONMA**[†a)], ***Member***, **Ryota ITO**[†], ***Nonmember***, ***and*** **Toshiaki NOSE**[†], ***Member***

SUMMARY In recent years, demand for smart windows with dimming and other functions has been increasing, e.g., polymer dispersed liquid crystals. Liquid crystal (LC) gels also have the potential for smart glass applications owing to their light-scattering properties. In this study, LC gels were prepared by mixing nematic LC (E7) with poly(9,9-di-n-octylfluorenyl-2,7-diyl) (PFO) as a gelator. The LC gel formed a dense PFO network as the concentration increased. The PFO network structure changed in response to the change in the cooling rate. High contrast ratio of light scattering was obtained for the LC gel device that was fabricated via the 2-wt%-doping of PFO and natural cooling. Furthermore, the PFO concentration and cooling rate were found to affect the response time of the LC gel device.

key words: *liquid crystal, liquid crystal gel, polyfluorene, smart window*

1. Introduction

In recent years, the demand for smart windows with light control and heat shielding functions in buildings and automobiles has increased [1], [2]. In addition, smart windows have potential applications as light-controlling and display devices [3]. Ordinary liquid crystal (LC) smart windows include polymer dispersed LCs (PDLCs) [4], [5] and polymer network LCs (PNLCs) [6], [7], well known for their excellent light-switching properties when voltage is applied. They are applicable to commercial devices [8], [9]. Smart windows using PDLCs and PNLCs can control light scattering by varying the refractive index difference between the LC monomer and polymer matrix [8]. However, the operating threshold voltage generally increases with the formation of a polymer matrix or network.

In many cases, the polymer network structure is formed via photopolymerization, while sol–gel transitions have also been adopted to construct the polymer network. Gels are generally classified as chemical or physical gels. LC gel devices, which exhibit controllable light-scattering properties under an applied voltage, have been extensively studied [10]–[15]. According to previous studies, the driving voltage of LC gel devices are comparable to that of pure nematic LC devices, that is, a few volts [12], [15]. Furthermore, the gel structure of physical gels can be easily broken and built up via heating and cooling processes by applying appropriate heating and cooling rates. This modifying function of the gel structure is attributed to the relatively weak interaction forces, such as π-π interactions and hydrogen bonds between polymer molecules. Therefore, physical gels have an advantage over chemical gels, formed by cross-linking through covalent bonds. Based on these features, LC gel devices are expected to be applicable to smart windows.

Thus far, LC gels have been generated by adding a polyfluorene polymer (F8BT) as a gelator [11], [13]. The fabricated LC gel device exhibited a light scattering function that is switchable at low driving voltage [14].

In this study, we used polyfluorene (PFO) as a gelator to form a physical gel network in an ordinary nematic LC, E7. The structure of the PFO network was first investigated by observing the E7/PFO gels with polarized light microscopy and fluorescence microscopy. Next, the transmittance and voltage characteristics were measured to determine the optimal PFO concentration to obtain a high contrast ratio. Finally, the response properties were measured, and the effect of the PFO network on the response time was analyzed based on observations using a polarized light microscope and the measured response curves.

2. Experimental Details

LC gels were prepared using nematic LC (E7, LCC, Japan) with a phase transition temperature of 60°C [14], [15]. Poly(9,9-di-*n*-octylfluorenyl-2,7-diyl) (PFO, Sigma-Aldrich, weight average molecular weight (M_W): $\geq 20,000$) was used as a gelator. The molecular structures of E7 and PFO are shown in Fig. 1. The LC gel cell was fabricated by sandwiching the LC gel layer between a pair of indium-tin-oxide (ITO)/glass substrates. A polyimide film (SE2170, Nissan Chemical) was used as an alignment film, and the cell gap was controlled using glass rod spacers (diameter: 10 μm). During the mixing process, a small amount of PFO powder was added to E7 (solvent) to obtain PFO concentrations of 0.2, 1, 2, and 3 wt%. Next, the solution was heated to 150–160°C and stirred (300 rpm) until the PFO powder dissolved. Subsequently the heated solution was injected into heated empty cells. Finally, the filled cells were cooled to 25°C at different cooling rates. For slow cooling (averaging 0.7°C/min), an electric furnace was used to control the cooling rate. For fast cooling (averaging 19°C/min), the cells were placed on a laboratory table at room temperature.

Manuscript received March 29, 2023.
Manuscript revised June 1, 2023.
Manuscript publicized August 10, 2023.

[†]The authors are with Department of Information Mechatronics, Akita Prefectural University, Yurihonjo-shi, 015–0055 Japan.
a) E-mail: mhonma@akita-pu.ac.jp

DOI: 10.1587/transele.2023DII0005

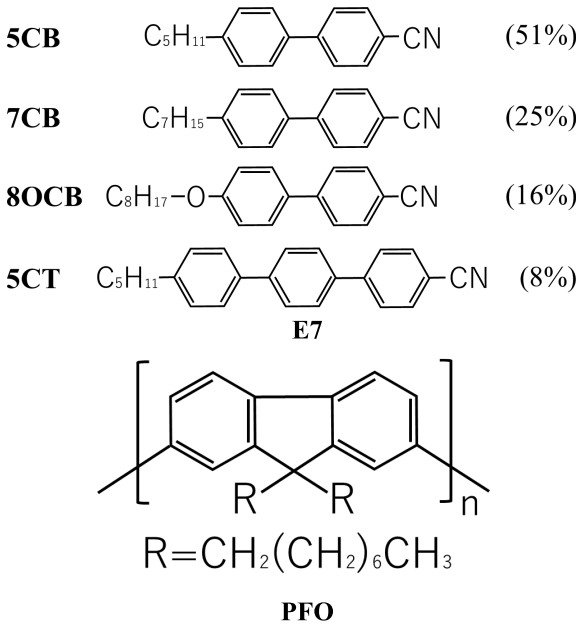

Fig. 1 Structural formulae of LC (E7: LCC, Japan) and gelator (PFO: Sigma-Aldrich).

3. Results and Discussion

3.1 Network Structures of LC Gels

We observed the LC gel cells using polarized light microscopy and fluorescence microscopy to examine the formed network of the gel. Figure 2 shows photographs captured without an applied voltage (polarization microscopy, at room temperature). The pinkish color originates from the birefringence of the nematic LC. In the case of 0.2-wt%-cell (Fig. 2 (a)), PFO aggregated and formed tiny clumps. In contrast, when the PFO concentration was 1 wt%, a coarse network structure was formed, as shown in Fig. 2 (b). A dense network structure was produced when the concentration was further increased to 2 wt% (Fig. 2 (c)). Furthermore, the network became denser when the PFO concentration increased to 3 wt%. In Figs. 2 (a) and 2 (b), the pinkish area corresponds to the pure LC area; that is, the color is generated by LC birefringence. A similar color was observed for 2 and 3 wt% (Figs. 2 (c) and 2 (d)), although the entire area was covered with the PFO network. This indicates that LC/PFO phase separation is induced, and the orientation of the LC molecules in the dense network is not entirely random but partially oriented.

Figure 3 shows an LC gel cell observed using a fluorescence microscope to reveal the spatial distribution of the PFO network. The dark areas represent the LCs, and the blue fluorescence areas correspond to the PFOs. When the PFO concentration was 0.2 wt% (Fig. 3 (a)), small clumps of PFO were recognized, whereas a coarse PFO network was formed when the concentration was 1 wt% (Fig. 3 (b)). In contrast, the 2- and 3-wt%-cells created almost uniform blue

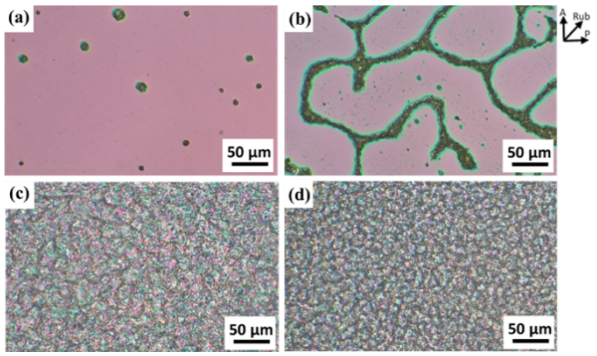

Fig. 2 Polarized light micrographs of PFO-doped cells at concentrations of (a) 0.2 wt%, (b) 1 wt%, (c) 2 wt%, and (d) 3 wt%.

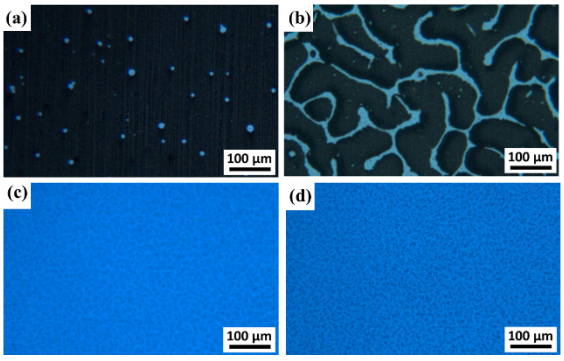

Fig. 3 Fluorescence micrographs of PFO-doped cells at concentrations of (a) 0.2 wt%, (b) 1 wt%, (c) 2 wt%, and (d) 3 wt%.

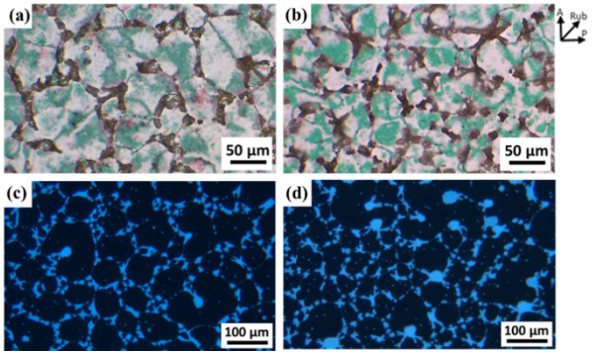

Fig. 4 Polarized light micrographs of (a) 2-wt%- and (b) 3-wt%-cells. Fluorescence micrographs at PFO concentrations of (c) 2 wt% and (d) 3 wt%. Both LC gel cells were fabricated under slow cooling conditions.

images (Figs. 3 (c) and 3 (d)). This indicates that the PFO network was densely entangled in the entire LC layer.

Figures 4 (a) and 4 (b) show polarization micrographs of the slow-cooled LC gel cells with PFO concentrations of 2 and 3 wt%, respectively. As is evident from these micrographs, the dense network structure in Figs. 2 (c) and 2 (d) was no longer generated in the case of slow cooling. Instead, PFO aggregated and formed larger clumps than that in the fast-cooled gel. Next, fluorescence microscopy was conducted to investigate the spatial distribution of the PFO network. Unlike the case of fast cooling (Figs. 3 (c) and

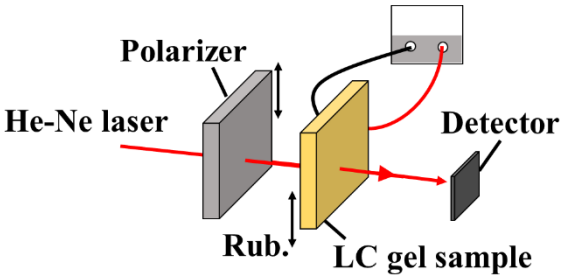

Fig. 5 Experimental setup for measuring transmittance and voltage characteristics of LC gel cells.

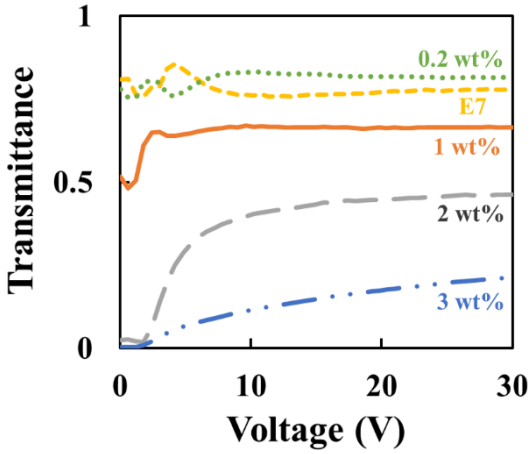

Fig. 6 T-V curves of LC gel cells with different gelator concentrations.

3 (d)), Figs. 4 (c) and 4 (d) show that the PFO has aggregated considerably, and the network structure was sparsely intertwined in the entire LC layer.

3.2 Transmittance-Voltage Characteristics

Next, the transmittance-voltage characteristics of the LC gel cells were measured using the experimental system (Fig. 5). The measurement system comprised a He-Ne laser (633 nm), polarizer, LC gel cell, and photodetector. An alternating current (AC) voltage of 0–30 V (1 kHz, sinusoidal) was applied across the LC gel cell. The polarization direction of the He-Ne laser was aligned with the rubbing direction. The transmitted light was detected using a photodiode (area: 10 × 10 mm) positioned 200 mm away from the cell. The polarization direction of the incident light was set parallel to the rubbing direction to maximize the light-scattering effect.

Figure 6 shows the transmittance-voltage (T-V) curves of LC gels with different gelator concentrations, in which we used a homogeneous orientation LC cell with a 10 μm cell gap. The LC cell was prepared under fast-cooling conditions. For the pure LC and 0.2 wt% cells, the transmittance was almost constant as the applied voltage increased, whereas the 1, 2, and 3 wt% cells exhibited an increasing tendency in the transmittance curve. This trend suggests that the LC director becomes perpendicular to the substrate surface and reduces index mismatch when the applied voltage increases.

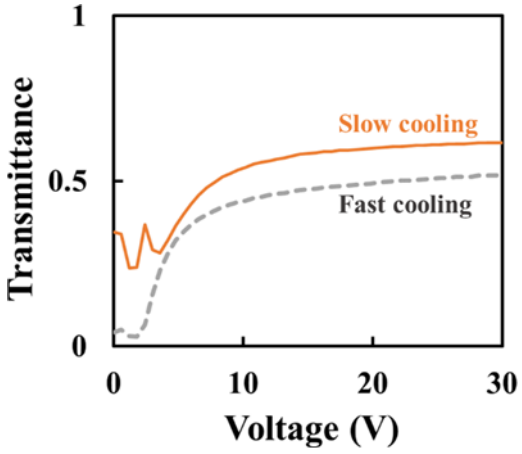

Fig. 7 T-V curves of LC gel cells fabricated at different cooling rates.

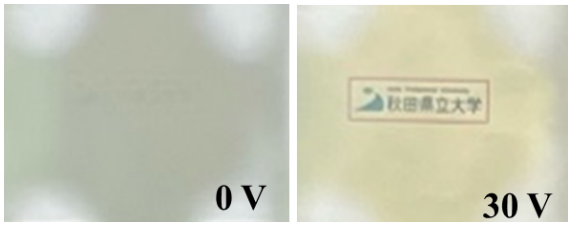

Fig. 8 Switching operation of light scattering of the fast-cooled LC gel cell with 2 wt% PFO. The cell gap was 10 μm.

Additionally, the transmittance decreased with increasing PFO concentration. Notably, the 2 wt% PFO cell yielded a good contrast ratio of $T_{30V}/T_{0V} = 19.4$.

Figure 7 shows the T-V curves of LC gel cells fabricated at different cooling rates without rubbing treatment. The PFO concentration was 2 wt%, and the cell gap was 10 μm. The transmittance of the slow-cooled cell (T_{slow}) was generally higher than that of the fast-cooled cell (T_{fast}) (Fig. 7). The difference between these transmittances ($\Delta T = T_{slow} - T_{fast}$) was significant at 0 V and decreased as the applied voltage increased. This difference, ΔT, is attributed to the formation of the dense network structure because the degree of the PFO aggregation changes with the cooling rate. In the fast-cooled cell, the dense PFO network strongly scatters the incident light when no voltage is applied. In contrast, the sparse distribution of the PFO network eases the light-scattering effect in the slow-cooled cell. Consequently, the contrast ratio of the fast-cooled cell ($T_{30V}/T_{0V} = 12.5$) is higher than that of the slow-cooled cell ($T_{30V}/T_{0V} = 1.8$). The highest contrast ratio is obtained for the 2 wt% concentration and the fast-cooled cell (Figs. 6 and 7). Moreover, the LC cells can be driven with threshold voltages as low as 2–3 V. Such low threshold voltage is frequently obtained in the LC gel devices.

Figure 8 presents photographs of the actual switching operation of the LC gel cell. When no voltage was applied, strong light scattering occurred. When a voltage of 30 V was applied, the transparency of the LC cell increased, and a printed paper sheet placed behind the LC cell became visible

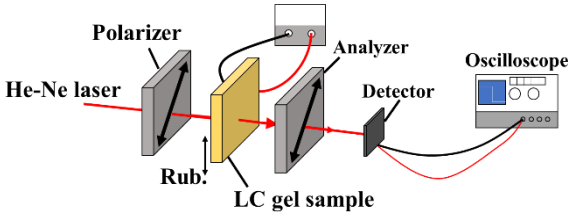

Fig. 9 Experimental setup for measuring response time of LC gel cell.

Table 1 Measured response times of LC gel cells.

Respose time	with analyzer		no analyzer	
	fast cooling	slow cooling	fast cooling	slow cooling
Rise (ms)	42	100	26	96
Decay (ms)	14	455	16	498

to the naked eye.

3.3 Response Properties

Finally, we investigated the response properties of the LC gel cells using the experimental setup shown in Fig. 9. The measurement system comprised a He-Ne laser (633 nm), a pair of polarizers (parallel Nicols), the LC gel cell, a photodetector, and an oscilloscope. The polarization direction of the incident light was set at a 45° angle to the rubbing direction. The transmitted light was detected using a photodetector (diameter: 0.9 mm) positioned 800 mm away from the cell. An AC voltage of V_{rms} = 3.54 V (1 kHz, sinusoidal) was applied to operate the LC gel cell, and the voltage amplitude was modulated with a frequency of 1 Hz. The transient light intensity curve was plotted using an oscilloscope. The response time was then evaluated from the measured curve.

Table 1 lists the response times when the PFO concentration was 3 wt%, and the cell gap was 10 μm. Both the rise and decay times were influenced by the cooling rate. The fast-cooled cell exhibited shorter response times than the slow-cooled cell for the rise and decay processes. This improvement in response time was attributed to the dense PFO network structure.

Figure 10 shows the response curves of LC gel cells with different PFO concentrations (0 and 3 wt%) and cooling rates. In the case of a pure E7 cell (Fig. 10 (a)), the light intensity fluctuated when the voltage was switched on or off, owing to the change in the LC molecular orientation. Conversely, the fluctuation in the response curve disappeared when the concentration was 3wt% (fast-cooled, Fig. 10 (b)). This is because of the dense PFO network structure (Fig. 2 (d)), which can restrict the movement of the LC director. Furthermore, the fluctuation reappeared when the LC gel cell was prepared under the slow-cooling conditions, even though the PFO concentration remained unchanged (3 wt%). We suspect that the sparsely distributed PFO network reduces the interaction between the LC molecules and PFO network, allowing for unconstrained movement of the LC molecules. Based on these findings, we conclude that the network structure significantly influences the fluctuation of

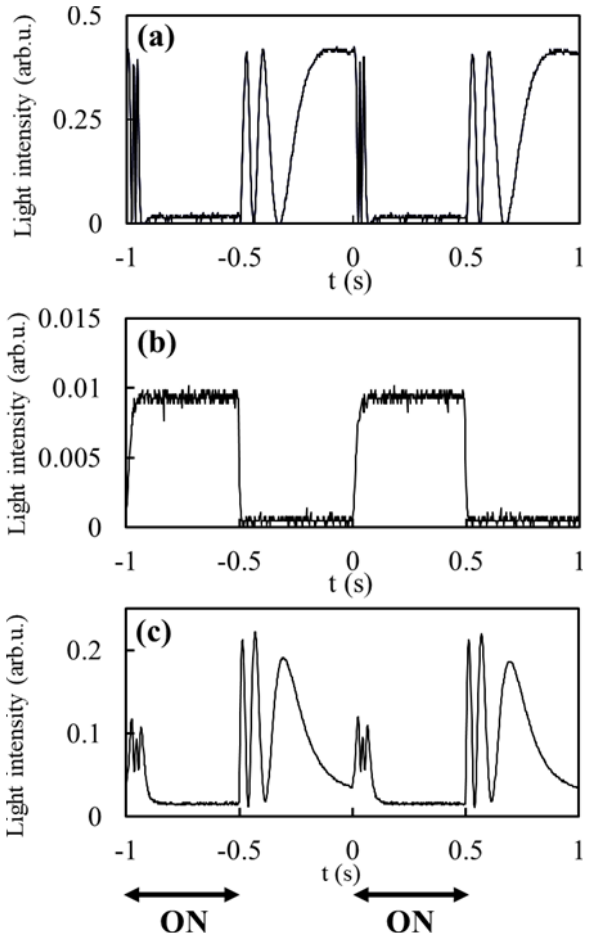

Fig. 10 Response curves of fabricated LC gel cells: (a) E7 (0 wt%), (b) 3 wt%, fast-cooling, and (c) 3 wt%, slow-cooling.

the response curve.

The pure E7 cell and slowly cooled cells (Figs. 10 (a) and 10 (c)) all showed low transmittance when a voltage was applied across the cell, irrespective of the use of parallel Nicols polarizers. This indicates that the applied voltage (V_{rms} = 3.54 V) is insufficient to fully align the LC director perpendicular to the LC layer. When the voltage was switched off, the transmittance in the slow-cooled cell (Fig. 10 (c)) gradually decreased with time. This decrease is attributed to the increasing prominence of the light-scattering effect as the LC director lays flat in the LC layer. Therefore, the slow-cooled cell (Fig. 10 (c)) operates in an intermediate mode between birefringence (Fig. 10 (a)) and light scattering (Fig.10 (b)).

4. Conclusion

LC gel cells with different gelator (PFO) concentrations and cooling rates were investigated in this study. It was found that the PFO concentration and cooling rate influenced the degree of PFO aggregation and the spatial distribution of the PFO network structure (sparse or dense distributions). A high contrast ratio (19.4) was obtained for a 2 wt% con-

centration and fast-cooling conditions. In the fabricated LC cells, the driving voltage required for switching the light-scattering effect was low (2–3 V), unlike ordinary PDLC cells. Furthermore, the formation of the dense PFO network leads to a good switching of light scattering and a short response time. Therefore, LC gel devices fabricated using appropriate PFO concentrations and cooling rates are suitable for various light-controlling devices, including smart windows.

References

[1] C.G. Granqvist, A. Azens, A. Hjelm, L. Kullman, G.A. Niklasson, D. Rönnow, M. Strømme Mattsson, M. Veszelei, and G. Vaivars, "Recent advances in electrochromics for smart windows applications," Solar Energy, vol.63, no.4, pp.199–216, 1998.
[2] Y. Zhao, H. Ji, M. Lu, J. Tao, Y. Ou, Y. Wang, Y. Chen, Y. Huang, J. Wang, and Y. Mao, "Thermochromic smart windows assisted by photothermal nanomaterials," Nanomaterials, vol.12, no.21, pp.3865–3881, 2022.
[3] D. Ge, E. Lee, L. Yang, Y. Cho, M. Li, D.S. Gianola, and S. Yang, "A robust smart window: reversibly switching from high transparency to angle-independent structural color display," Adv. Mater., vol.27, pp.2489–2495, 2015.
[4] J.W. Doane, N.A. Vaz, B.-G. Wu, and S. Žumer, "Field controlled light scattering from nematic microdroplets," Appl. Phys. Lett., vol.48, no.4, pp.269–271, 1986.
[5] J.L. West, "Phase separation of liquid crystals in polymers," Mol. Cryst. Liq. Cryst., vol.157, no.1, pp.427–441, 1988.
[6] I. Dierking, "Polymer network–stabilized liquid crystals," Adv. Mater., vol.12, no.3, pp.167–181, 2000.
[7] R. Yamaguchi, K. Inoue, and R. Kurosawa, "Effect of liquid crystal material on polymer network structure in polymer stabilized liquid crystal cell," J. Photopolym. Sci. Technol., vol.29, no.2, pp.289–292, 2016.
[8] V. Sharma, P. Kumar, and K.K. Raina, "Simultaneous effects of external stimuli on preparation and performance parameters of normally transparent reverse mode polymer-dispersed liquid crystals—a review," J. Mater. Sci., vol.56, no.34, pp.18795–18836, 2021.
[9] D. Cupelli, F.P. Nicoletta, S. Manfredi, M. Vivacqua, P. Formoso, G. De Filpo, and G. Chidichimo, "Self-adjusting smart windows based on polymer-dispersed liquid crystals," Solar Energy Mater. Solar Cells, vol.93, pp.2008–2012, 2009.
[10] T. Cardinaels, Y. Hirai, K. Hanabusa, K. Binnemans, and T. Kato, "Europium (III)-doped liquid-crystalline physical gels," J. Mater. Chem., vol.20, no.39, pp.8571–8574, 2010.
[11] J.-W. Chen, C.-C. Huang, and C.-Y. Chao, "Supramolecular liquid-crystal gels formed by polyfluorene-based π-conjugated polymer for switchable anisotropic scattering device," ACS Appl. Mater. Interfaces, vol.6, no.9, pp.6757–6764, 2014.
[12] J.-W. Chen, Y.-Y. Kuo, C.-R. Wang, and C.-Y. Chao, "The formation of supramolecular liquid-crystal gels for enhancing the electro-optical properties of twisted nematic liquid crystals," Org. Electron., vol.27, pp.24–28, 2015.
[13] J.-W. Chen, Y.-Y. Kuo, K.-T. Chen, C.-R. Wang, and C.-Y. Chao, "The function of self-assembled polyfluorene-based π-conjugated supramolecular structures formed in twisted nematic liquid crystals," Mol. Cryst. Liq. Cryst., vol.611, no.1, pp.139–145, 2015.
[14] Y.-X. Chen and J.-S. Hsu, "Ultra-low switching reverse mode liquid crystal gels," Opt. Express, vol.28, no.18, pp.26783–26791, 2020.
[15] A. Yagi, M. Honma, R. Ito, and T. Nose, "Optical properties of nematic liquid crystal/ polyfluorene gel devices," Proc. 29th International Display Workshops, LCTp1-8L, Fukuoka, Dec. 2022.
[16] J. Peláez and M. Wilson, "Molecular orientational and dipolar correlation in the liquid crystal mixture E7: a molecular dynamics simulation study at a fully atomistic level," Phys. Chem. Chem. Phys., vol.9, no.23, pp.2968–2975, 2007.

Asuka Yagi received her B.E. degree from Akita Prefectural University in 2021. She has been involved in the development of novel liquid crystal gel devices as a student in the master's course at Akita Prefectural University.

Michinori Honma received master's and doctoral degrees of engineering from Akita University in 1997 and 2000, respectively. Since 2000, he has been engaged in research on liquid crystal devices at Akita Prefectural University. From April 2000 to September 2004, he was a research associate, and from October 2004, he has been an associate professor. He is a member of the Optical Society, the Institute of Electronics, Information and Communication Engineers, the Japan Society of Applied Physics, the Optical Society of Japan, and the Japanese Liquid Crystal Society. He has been engaged in research works for liquid crystal optical and MMW device applications.

Ryota Ito received B.S. degrees of engineering from Akita Prefectural University in 2004. He received his M.S. degree in electronic engineering from Tohoku University in 2006. From 2006 to 2012, he was a research associate at Akita Prefectural University. He then obtained his Ph.D. in electronics engineering from Osaka University in 2012. Since 2012, he has been an assistant professor at Akita Prefectural University, where he has been engaged in research on THz waves and liquid crystal devices.

Toshiaki Nose received his B.S. degree in electrical engineering and M.S. degree in electronic engineering from Tohoku University, Sendai, Japan, in 1983 and 1985, respectively. From 1985, he was a Research Associate at Akita University, Akita, Japan, and received his Ph.D. in electronics engineering from Tohoku University in 1995. Since 1999, he has been a Professor at Akita Prefectural University, Yurihonjyo, Japan. He has been engaged in research works for liquid crystal optical device applications, and recently extended his research interests to millimeter-waves and THz waves.